Hindawi
Advances in Civil Engineering
Volume 2020, Article ID 8328412, 10 pages
https://doi.org/10.1155/2020/8328412

Research Article

Study on the Applicability of Needle/Cone Penetration Experiment for Asphalt-Rubber

Zechen Yao,[1] **Renfeng Yang**,[1] **Zhonglin Liu**,[2] **Haichao An**,[1] **Qingzhe Zhang**,[1] **and Wei Yuan**[1]

[1]*School of Construction Machinery, Chang'an University, Xi'an 710064, China*
[2]*Hebei Provincial Transportation Department, Shijiazhuang 050000, China*

Correspondence should be addressed to Zechen Yao; 372896087@qq.com

Received 25 October 2019; Revised 31 August 2020; Accepted 1 September 2020; Published 24 September 2020

Academic Editor: Hui Yao

In order to quantitatively study the applicability of needle/cone penetration experiment for asphalt-rubber (AR), the dynamic model of needle/cone in penetration process was established based on the *Kelvin* model, and the different impacts of crumb rubber (CR) particles on needle/cone penetration depth were analyzed using *Matlab*. The probability of needle/cone contacting CR particles in penetration process was statistically calculated. AR binders with different CR particle sizes were observed using scanning electron microscope (SEM) and prepared for testing needle/cone penetration. The results showed that the solid-liquid two-phase feature of AR binders gradually weakened with the reduction of CR particle size. At the same viscoelastic parameters, CR particles had little impact on cone penetration depth when cone contacted CR particles. The probability of cone contacting CR particles was close to 100% in penetration process while that of needle was around 50%. The standard deviations of the needle penetration experimental results for AR binders with #20, #30, #40, #60, and #80 mesh CR were 4.0, 3.8, 2.8, 1.1, and 1.1 times of cone penetration, respectively. This study shows that the cone penetration experiment has a significant advantage in evaluating the consistency of the AR binder with coarse CR.

1. Introduction

Currently, nearly 1.5 billion waste tires are discarded around the world each year and the number is still increasing sharply [1]. Waste tires consist of long polymer chains, most of which are crosslinked with sulfur bridges. It is very difficult to recover and recycle waste tires [2, 3]. The disposal of used tires is a worldwide problem, and burying or burning is the general treatment. Hence, waste tires are called "black pollution" [4, 5]. Asphalt-rubber (AR) is a new material which is made by adding crumb waste tire rubber into asphalt. On the one hand, it can reduce an amount of waste tires, and on the other hand, it can improve the road performance of asphalt by using natural rubber and carbon black in waste tires [6, 7]. The AR binder's evaluation indexes are not unified across the world in AR application process, but their core technical indexes are viscosity, needle/cone penetration, soften point, and elastic recovery rate.

Needle/cone penetration is an important index to evaluate the AR binder's consistency, which represents the soft (hard) degree of the binder. However, there are some differences between these two evaluation indexes. The needle penetration experiment is carried out using test needle, which is mainly reflecting the shearing effect of the needle tip on sample, and few AR binders can be tested. For cone penetration, the cone tip has the shearing effect on sample which is similar to the needle penetration, while the cone body also has compressive stress on the sample, and more AR binders can be tested. Choosing the appropriate test method can reduce the variability of the experimental results and also reduce the test times and cost. Moreover, the real quality of AR binders can be reflected. The needle penetration at 25°C following SBS modified asphalt' evaluation system is mostly used in AR local technical standards in China [8]. Due to AR's solid-liquid two-phase property, it often contains large crumb rubber (CR) particles, which may

have an impact on penetration experimental results. Therefore, in some places, such as California and Texas in the United States, needle penetration is replaced by cone penetration, and ASTM D6114 stipulates that needle penetration experiment at 25°C and 4°C should be combined to avoid inaccurate results [9]. Exploring the applicability of needle/cone penetration experiment for the AR binder is of great significance to improve the AR binder's product quality and popularize its applications.

There have been some studies on needle/cone penetration experiments. Huang and Pauli et al. carried out experiments using eight different AR binders, and the needle penetration experimental results were highly discrete [10]. The study of Yang et al. showed that cone penetration may be more suitable for evaluating the AR binder [11]. Hao et al. thought that there will be a large deviation if needle penetration experiment was used to test the AR binder with coarse CR [8]. Wang et al. proposed that cone penetration at 25°C and shear strength were more suitable for evaluating the AR binder's consistency [12]. Al-Omari et al. and Mashaan and Karim studied the effect of CR content on needle penetration experiment [13, 14]. The results showed that the needle penetration at 25°C decreased significantly and its variability increased with CR content. Although great progress has been made in the research on the AR binder's penetration experiment, there are still some limitations. Most of these studies have only carried out simple penetration experiments for AR binders. At present, there is a lack of analysis on the applicability of AR binder consistency experiment from the point of view of CR modification mechanism and theoretical analysis.

Based on the modification mechanism of coarse/fine CR, this paper emphatically analyzed the needle/cone penetration experimental process for the AR binder with coarse CR which shows obvious solid-liquid two-phase feature macroscopically. Starting with the mechanical analysis of needle/cone in penetration process, the needle/cone's dynamic model was established based on visco-elasticity constitutive relationship, and the differential equations of penetration depth varying with time were obtained. According to statistical principle, the probability of needle/cone contacting CR particles in penetration process was calculated and the difference of testing mechanism between them was explored. Finally, the needle/cone penetration experiments on AR binders with different particle sizes were carried out to verify the correctness of theoretical analysis. This paper can provide theoretical support for the superiority of cone penetration to evaluate the AR binder with coarse CR.

2. Experiments

2.1. Materials. The asphalt in this research was a pure asphalt binder with 90 penetration grades received from SK, Shell, and East Sea, respectively. Ambient grinding CR of #20, #30, #40, #60, and #80 mesh produced by Shaanxi Expressway, Hunan HeDeLi, and Xian ZhongXuan was used to prepare AR binders. The main technical parameters are shown in Tables 1 and 2.

Table 1: Main technical indexes of base asphalt.

Experiment item	SK90#	Shell 90#	East Sea 90#
Density (25°C)/g·cm^{-3}	1.031	1.032	1.034
Needle penetration experiment (25°C)/0.1 mm	85	87	85
Force-ductility (15°C)/cm	>100	>100	>100
Softening point (°C)	46.0	45.5	46.0

Table 2: Main technical indexes of CR.

Experiment item	Shaanxi Expressway	Hunan HeDeLi	Xian ZhongXuan
Density/ (g·cm^{-3})	1.17	1.19	1.18
ω_{water} (%)	0.75	0.81	0.78
ω_{metal} (%)	0	0.01	0
ω_{fiber} (%)	0.01	0	0.02
Ash (%)	6.00	5.02	7.20
Acetone extractives (%)	6.18	6.13	3.86
Carbon black (%)	28	28	29
Rubber hydrocarbon (%)	61	57	57

2.2. Preparation of AR Binders. The AR binders were prepared by wet process. The #20, #30, #40, #60, and #80 mesh CR (20% by the weight of asphalt) from Shaanxi Expressway, Hunan HeDeLi, and Xian ZhongXuan were mixed with base asphalt from SK, Shell, and East Sea, respectively, to prepare AR binders. The AR binders were obtained by adding CR to the base asphalt, which was melted at 80°C–90°C in an oven previously. Manually stir for 5 min to predistribute CR in base asphalt, and then blend by using a high-speed mixer (at about 1000 rpm) with 180°C (±5°C) for 45 min following ASTM D6114-19 [9].

2.3. Experimental Methods. In order to explore the distribution of fine CR in base asphalt, the AR binders (prepared by East Sea asphalt and Xian ZhongXuan CR) with #40, #60, and #80 mesh CR were observed using FEI Quanta FEG 250 FESEM following GB/T 16594-08 [15]. Every batch of AR binders was tested ten times for needle/cone penetration at 25°C using an SD2801C digital penetration meter following GB/T 4509-10 [16].

3. Results and Discussion

3.1. Mechanical Model of Needle/Cone in Penetration Process

3.1.1. Dispersion Analysis. Figure 1 shows the AR binders with different CR particle sizes. Obvious CR particles can be observed in AR binders with #20, #30 CR, and tiny CR particles distributing in the AR binder with #40 CR can also be observed. However, CR particles cannot be observed in AR binders with #60, #80 CR macroscopically. The SEM images of AR binders with #40, #60, and #80 CR are shown in Figure 2. The silver particles are CR in picture. As shown in Figure 2(a), the AR binder with #40 CR has many obvious silver particles, which shows distinct solid-liquid two-

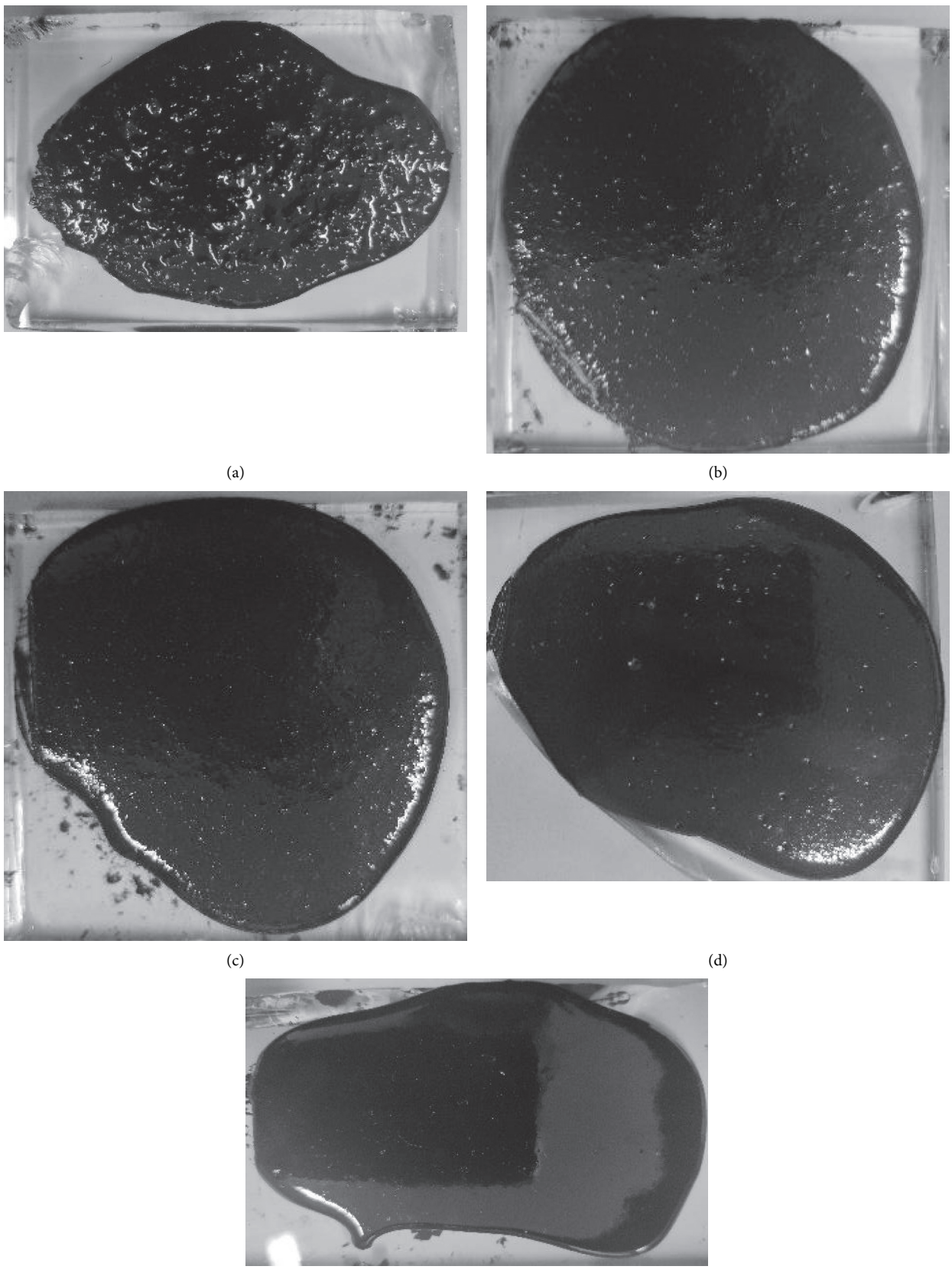

Figure 1: AR binders with different CR particle sizes. (a) AR with #20 CR, (b) AR with #30 CR, (c) AR with #40 CR, (d) AR with #60 CR, and (e) AR with #80 CR.

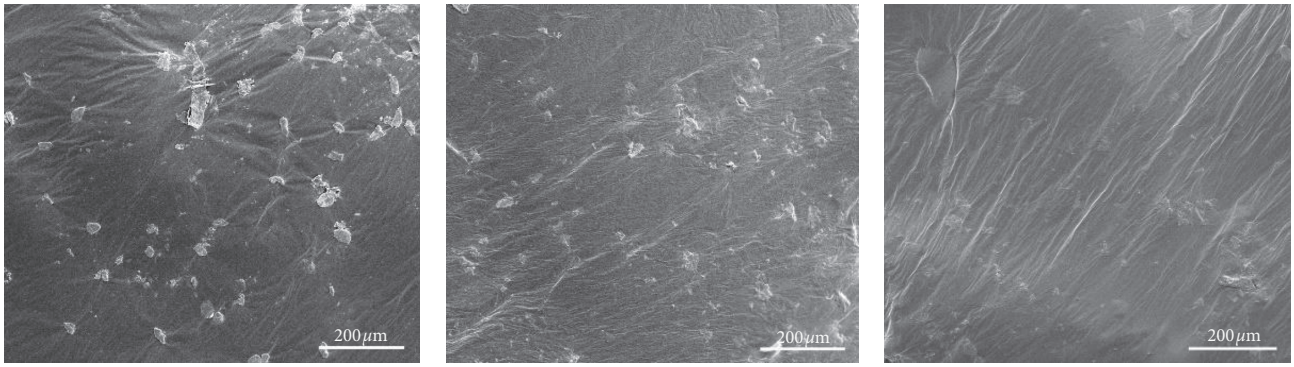

Figure 2: SEM images of AR binders with different CR particle sizes. (a) AR with #40 CR, (b) AR with #60 CR, and (c) AR with #80 CR.

phase feature. With the reduction of CR particle size, the AR binder's solid-liquid two-phase feature gradually weakens. In Figure 2(c), obvious CR particles in the AR binder with #80 CR cannot be observed under current magnification. In other words, it is approximated to a single-phase body. The range of coarse rubber particles was #40 mesh and below, and the range of tiny rubber particles was above #40 mesh. Therefore, when the consistency of the AR binder with fine CR was tested, the tiny CR particles may do not have a significant impact on experimental results due to it is approximated to a single-phase body. However, the deviation might be caused by the existence of larger CR particles when the consistency of the AR binder with coarse CR was tested.

Aiming at the AR binder with coarse CR, this section discusses the quantitative impact of needle/cone contacting CR particles on penetration depth in experimental process to compare the applicability of needle/cone penetration through establishing a dynamic model.

Figure 3 shows the needle/cone penetration experimental results at 25°C on AR binders with #20 mesh CR (produced by East Sea asphalt and ZhongXuan CR). Compared with cone penetration, needle penetration experimental results fluctuate greatly with range (1.19 mm) and standard deviation (3.7), which indicate that the existence of CR particles is easy to cause deviation for needle penetration results. The cause is that CR modulus is greater than asphalt at 25°C. If needle contacts CR particles in penetration process, the experimental results are small; on the contrary, they are large. This is consistent with observation results of SEM images and other literature studies' conclusions [8, 17, 18].

The penetration depth is considered to be closely related to the moment of needle contacting CR particles. In other words, the final penetration depth is shallow when needle contacts CR particles in the early stage of penetration process; the final penetration depth is deep when needle contacts CR particles in the later stage of penetration process. Therefore, the maximum depth 5.22 mm means that the needle did not contact CR particles at all; while the minimum depth 4.03 mm means that the needle contacted CR particles in the early stage of penetration process; middle range is from 4.03 mm to 5.22 mm, which means that needle contacted CR particles at some point in the middle.

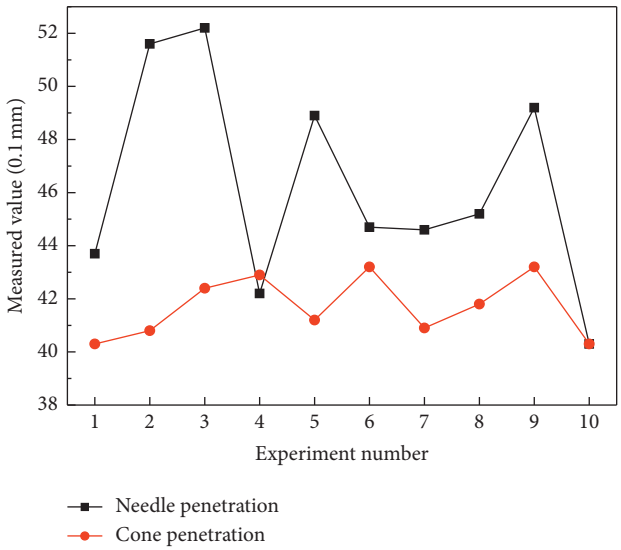

Figure 3: The needle/cone penetration experimental results of AR binders with #20 CR.

3.1.2. Axial Resistance Model. The geometric structure of needle/cone [16] is shown in Figures 4 and 5. The needle/cone was assumed to move vertically during penetration process. The process can be divided into two stages.

Stage 1 ($x < l$): as shown in Figure 6, only the needle tip contacts the AR binder, and the resistance is concentrated on the conical surface. Here, l is the vertical length of the needle tip; x is the penetration depth; p is the normal stress on the conical surface in the needle tip; f is the shear stress on the conical surface in the needle tip; and Φ is the half-angle of the needle tip.

The infinitesimal axial resistance of the needle is

$$dF_1 = (p \sin \phi + f \cos \phi) \mathrm{d}s. \quad (1)$$

The axial resistance is

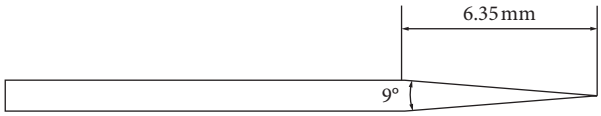

Figure 4: Needle.

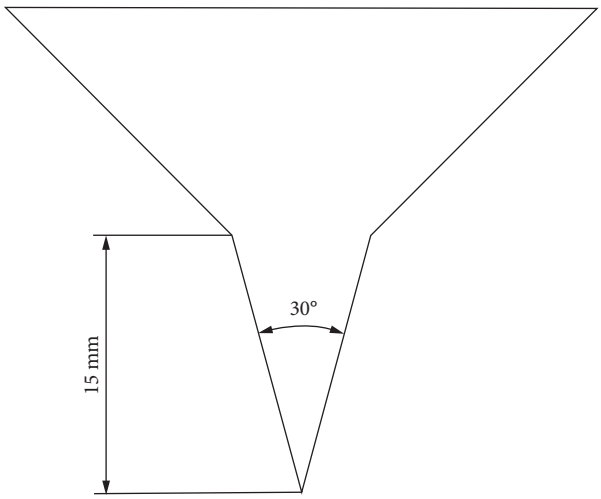

Figure 5: Cone.

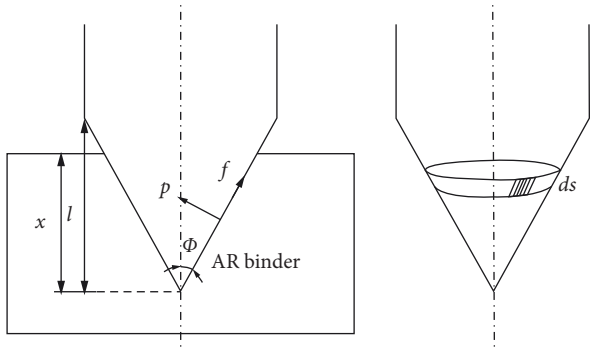

Figure 6: Mechanical analysis of stage 1.

$$F_1 = \iint \mathrm{d}F_1 = \iint (p\sin\phi + f\cos\phi)\mathrm{d}s = \pi x^2 \frac{\tan\phi}{\cos\phi}(p\sin\phi + f\cos\phi). \tag{2}$$

Stage 2 ($x > l$): the needle's conical and cylindrical surfaces are both subjected to resistance, and the mechanical analysis is shown in Figure 7. The q is shear stress on the cylindrical surface in the needle cylinder. The total axial resistance is

$$F = F_1 + F_2 = \pi l^2 \frac{\tan\phi}{\cos\phi}(p\sin\phi + f\cos\phi) + 2\pi q l \tan\phi (x - l), \tag{3}$$

where F_1 is the axial resistance of the conical surface; F_2 is the axial resistance of cylindrical surface; and F is the total axial resistance. According to (2) and (3), the axial resistance model of the needle in penetration process is obtained. It can

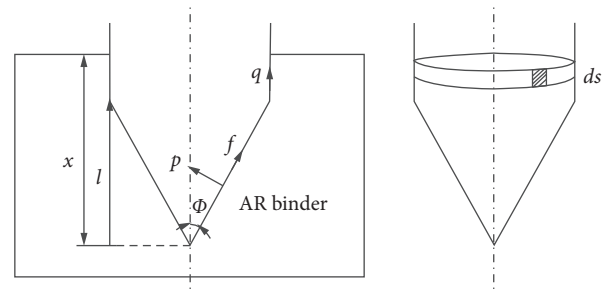

Figure 7: Mechanical analysis of stage 2.

be seen that p, q, and f are impacted by the AR binder's viscoelasticity. In order to easily solve the equations, the *Kelvin* model is used, and the constitutive relationship is shown in Figure 8: $\sigma = E\varepsilon + \eta\dot{\varepsilon}$.

As shown in Figure 9, the displacement x is decomposed:

$$F_1 = \pi x^2 \frac{\tan\phi}{\cos\phi}\left((\eta_1\dot{x} + E_1 x)\sin^2\phi + (\eta_2\dot{x} + E_2 x)\cos^2\phi\right),$$

$$F = \pi l^2 \frac{\tan\phi}{\cos\phi}\left((\eta_1\dot{x} + E_1 x)\sin^2\phi + (\eta_2\dot{x} + E_2 x)\cos^2\phi\right) + 2\pi l \tan\phi\,(\eta_3\dot{x} + E_3 x)(x - l). \tag{4}$$

The cone analysis process is similar to that of the needle except its geometric parameters are changed. In penetration process, needle/cone may contact CR particles. Because CR particles absorb the light component of asphalt in reaction process, it is no longer a pure elastomer [19]. In order to simplify the analysis, CR is regarded as a viscoelastic body whose modulus is higher than that of the AR binder.

3.1.3. Dynamic Model. According to mechanical analysis in Section 3.1.2 and experimental results in Section 3.1.1, the dynamic model of needle penetration process is established. Since penetration depth is shallow (<6.35 mm), analysis in stage 2 is unnecessary. According to Newton's second law of motion, the equation is obtained as follows when the needle is loaded by gravity:

$$mg - \pi x^2 \frac{\tan\phi}{\cos\phi}\left((\eta_1\dot{x} + E_1 x)\sin^2\phi + (\eta_2\dot{x} + E_2 x)\cos^2\phi\right) = m\ddot{x}. \tag{5}$$

According to the analysis in Section 3.1.1, maximum penetration depth 5.22 mm represents that the needle did not contact CR particles. The minimum penetration depth 4.03 mm means that the needle contacted CR particles in a short time, which is assumed at 0.5 s. The increase of modulus is used to simulate the needle contacting CR particles. As shown in Table 3, using *Matlab*, η_1, η_2, E_1, and E_2 are fitted by final penetration depth 5.22 mm, and η_1^*, η_2^*, E_1^*, and E_2^* are fitted by final penetration depth 4.03 mm when the needle contacts CR particles at 0.5 s.

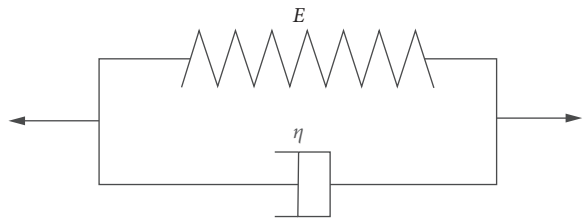

Figure 8: *Kelvin* model.

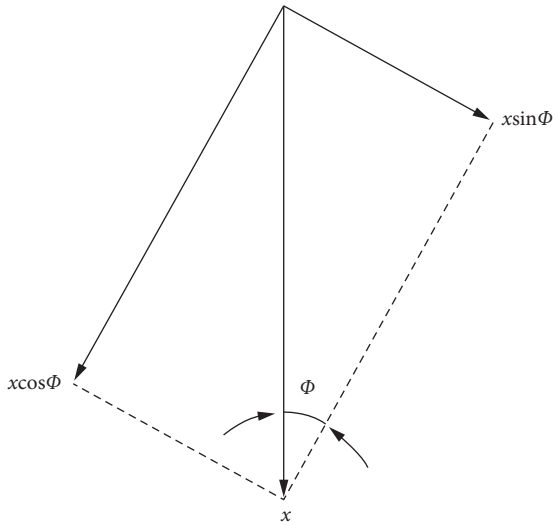

Figure 9: Displacement x decomposition.

Table 3: Viscoelastic parameters (the *Kelvin* model).

η_1	η_2	E_1	E_2	η_1^*	η_2^*	E_1^*	E_2^*
0.468	0.468	0.0468	0.0468	0.69	0.69	0.069	0.069

Matlab is used to solve (5). Figure 10(a) shows the variation of penetration depth and velocity with time whether the needle contacts CR particles at 0.5 s, 1 s, 1.5 s, and 2 s or not. Figure 10(b) shows the cone penetration process at the same viscoelastic parameters. Dashed lines represent the penetration depth, and solid lines represent the penetration velocity. As shown in Figures 10(a), 10(b), when the needle/cone contacts CR particles whose modulus is higher, the displacement and velocity curves change suddenly.

Table 4 shows the needle/cone's final penetration depth at the different moments of contacting CR particles. The difference between needle/cone final penetration depth without contacting CR and that contacting CR at 0.5 s is 1.19 mm and 0.89 mm, respectively. It shows that the cone penetration depth is less impacted by CR particles at the same viscoelastic parameters compared with the needle, and the situation is similar when the needle/cone contacts CR particles at other moments. This could be explained by the fact that cone volume is larger and heavier, and the increase of axial resistance caused by cone contacting CR particles with higher modulus has relatively little impact on final penetration depth in penetration process compared with the needle. Therefore, it may be more suitable for evaluating the AR binder with coarse CR which presents obvious solid-liquid property.

3.2. Probability Analysis in Penetration Experiments. On the one hand, the influence of coarse CR particles on the penetration experimental results is reflected in the difference of final penetration depth between the needle/cone contacting CR particles or not. On the other hand, the influence is related to the probability of needle/cone contacting CR particles. Hence, it is necessary to analyze the probability of needle/cone contacting CR particles in experiment process.

3.2.1. Probability Analysis of Needle Contacting CR Particles. According to experimental results in Section 3.1.1, it is assumed that #20 mesh CR particles (20% by the weight of asphalt) swell twofold [20] in reaction process and are randomly distributed in base asphalt. CR particle's shape is considered to be spherical. Maximum needle penetration depth 5.22 mm is used to calculate the probability of needle contacting CR particles. The related parameters of probability calculation are shown in Table 5.

The volume of the needle inserting into sample dish is

$$V_1 = \left(\frac{1}{3}\right)\pi L_1 (L_1 \tan \Phi_1)^2. \tag{6}$$

The volume of each CR particle is

$$V_R = \left(\frac{8}{3}\right)\pi \left(\frac{d}{2}\right)^3. \tag{7}$$

The volume of sample dish is

$$V_S = \pi H \left(\frac{D}{2}\right)^2. \tag{8}$$

The volume of total CR particles is

$$V_{RS} = 2 \times \frac{V_S/\rho_r}{(1/\rho_a) + (1/\rho_r)}. \tag{9}$$

In order to accurately calculate the probability of the needle contacting CR particles, each CR particle volume is regarded as a minimum unit and other volumes are divided according to the minimum unit. The total number of units is

$$N_s = \frac{V_S}{V_R}. \tag{10}$$

The number of units of needle penetration volume is

$$N_1 = \frac{V_1}{V_R}. \tag{11}$$

The number of units of all CR particles volume is

$$N_R = \frac{V_{RS}}{V_R}. \tag{12}$$

According to (6)–(12) and Table 5, the probability that there are no CR particles in needle penetration volume is

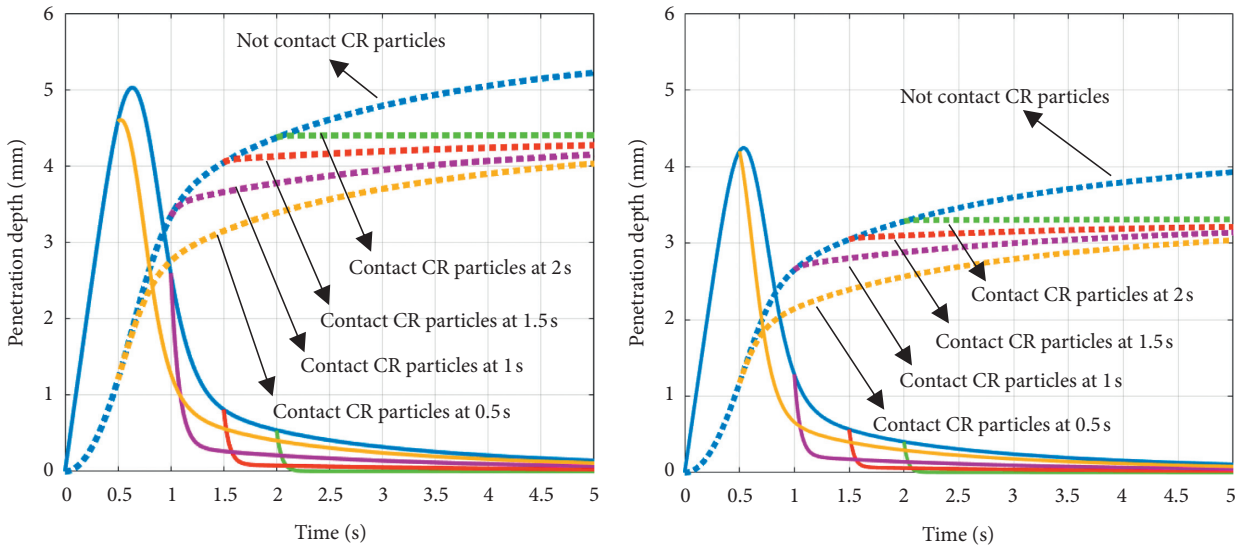

Figure 10: Needle penetration process. (a) Needle penetration process. (b) Cone penetration process.

Table 4: Final penetration depth of needle/cone contacting CR particles at different moments.

The moment of contacting CR particles (s)	No	0.5 s	1 s	1.5 s	2 s
Final penetration depth of needle (mm)	5.22	4.03	4.15	4.27	4.40
Final penetration depth of cone (mm)	3.93	3.04	3.14	3.21	3.31

Table 5: Parameters of probability calculation.

Needle penetration depth L_1	5.22 mm
Cone penetration depth L_2	4.32 mm
Half-angle tip of needle Φ_1	4.5°
Half-angle tip of cone Φ_2	15°
#20 mesh CR diameter d	0.83 mm
Sample dish diameter D	55 mm
Sample dish depth H	35 mm
Density of asphalt ρ_a	1.031 g·cm^{-3}
Density of CR ρ_r	1.17 g·cm^{-3}

$$p_1 = \prod_{N_s - N_R}^{N_s} \frac{i - N_1}{i} \times 100\% = 57.77\%. \quad (13)$$

From (13), the probability of needle contacting CR particles in penetration process is 42.23%. In other words, the needle is easy to contact CR particles or not in penetration experiment, which may impact penetration experimental results.

3.2.2. Probability Analysis of Cone Contacting CR Particles. Similar to the analysis in Section 3.2.1, the maximum cone penetration depth 4.32 mm was used to calculate the probability of cone contacting CR particles in penetration process. The volume of cone inserting into sample dish is

$$V_2 = \left(\frac{1}{3}\right)\pi L^2 \left(L^2 \tan \Phi_2\right)^2. \quad (14)$$

The number of units of cone penetration volume is

$$N_2 = \frac{V_2}{V_R}. \quad (15)$$

According to (7)–(10), (12), (14), and (15) and parameters in Table 5, the probability that there are no CR particles in cone penetration volume is

$$p_2 = \prod_{N_s - N_R}^{N_s} \frac{i - N_2}{i} \times 100\% = 2.72\%. \quad (16)$$

From (16), the probability of cone contacting CR particles is 97.28%. In other words, there is a small probability that the cone does not contact CR particles in penetration process. This may be also one of the causes why the dispersion of cone penetration experimental results is far less than that of needle penetration.

As shown in Figure 11, in order to clearly show the difference of the needle and cone penetration process, the distribution of spherical CR particles with double expansion was randomly generated using *Matlab* (sample size: 10 mm × 10 mm × 10 mm; content: 20%). Since the needle tip is fine and volume is small, the needle is easy to contact CR particles or not in penetration process, which is easy to impact experimental results. It is worth noting that either the needle contacts CR particles (the penetration depth is shallow) or not (the penetration depth is deep) cannot really evaluate the consistency of the AR binder with coarse CR. The AR binder as a kind of the solid-liquid two-phase miscible system, both its liquid-phase and solid-phase represent part of the AR binder's property. If the two

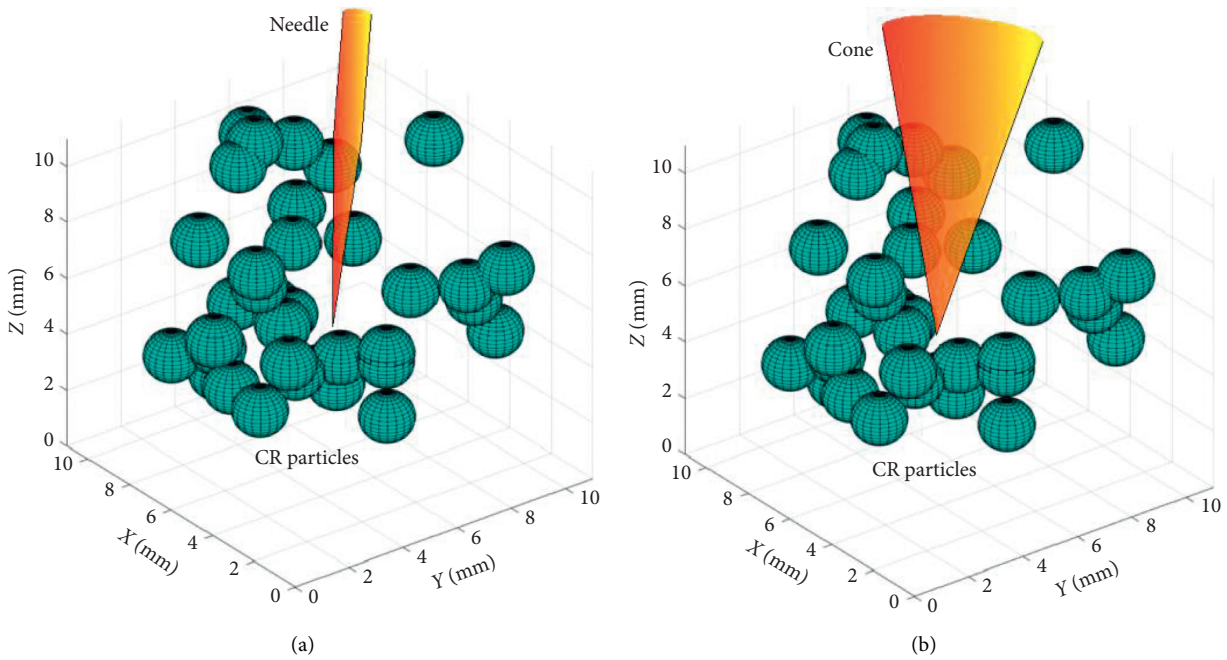

Figure 11: Experimental penetration process. (a) Needle penetration process. (b) Cone penetration process.

phases cannot be reflected, this evaluation method may have some limitations. Cone penetration process is shown in Figure 11(b), and cone is easy to contact multiple CR particles at the same time due to its larger tip angle and volume. On the one hand, more AR binder samples can be tested, and on the other hand, cone can not only produce a shear effect which is similar to the needle's effect on the AR binder but also produce compressive stress on the AR binder. Evaluating the AR binder's consistency with the compressive effect of larger contact area can reduce the influence of the solid-liquid phase on experimental results. Moreover, this testing method is more about the evaluation of elastic property of AR binder material itself. Hence, it may be more suitable for evaluating the AR binder with coarse CR which has obvious solid core.

3.3. Needle/Cone Penetration Experimental Results. As shown in Figure 12, with the increase of the CR mesh number, the standard deviations of the needle penetration experimental results decrease sharply, while the cone penetration results decrease slightly. The means of standard deviations of needle/cone penetration experimental results on AR binders with #20~80 CR are calculated to be 4.8/1.2, 4.2/1.1, 2.2/0.8, 0.8/0.7, and 0.8/0.7, respectively. The standard deviations of needle penetration are 4.0, 3.8, 2.8, 1.1, and 1.1 times of cone penetration, respectively.

For the AR binders with coarse CR (#40 mesh or lower), needle penetration experimental results are impacted easily by obvious CR particles. With the increase of the CR mesh number, the desulfurization and degradation of CR particles in reaction process are gradually intensified and the solid-liquid two-phase property of the AR binder is weakened. Hence, the stability of needle penetration experimental results is gradually improved. However, cone penetration experiment has a good applicability for the AR binder with both coarse and fine CR. The cone penetration experiment has a significant advantage for evaluating the AR binder with coarse CR (#40 mesh or lower), which also verifies the results of SEM observation and theoretical analysis.

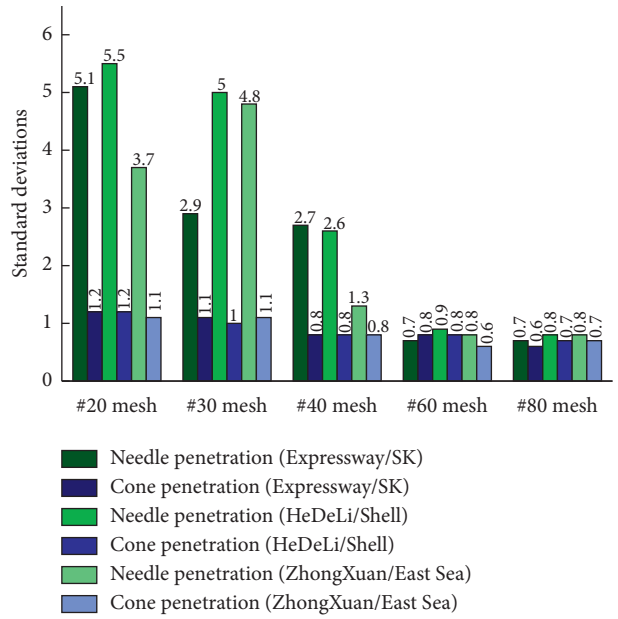

Figure 12: Standard deviations of the needle/cone penetration experimental results at 25°C for AR binders.

4. Conclusions

Aiming at large variability may appear in experimental results of AR needle penetration, based on viscoelastic model, probability analysis, and experiments, the applicability of needle/cone penetration experiment was analyzed. It is concluded that the cone penetration has a significant advantage in evaluating the consistency of the AR binder with coarse CR particles. The key findings are as follows:

(1) Obvious CR particles still exist in the AR binder with coarse CR after physical and chemical reactions of swelling and desulfurization degradation, which show distinct solid-liquid two-phase property. With the increase of the CR mesh number, CR's specific surface area increases gradually and its desulfurization and degradation reaction occupy more weight. Hence, there are no obvious CR particles under SEM, which may not impact the penetration experimental results.

(2) Compared with needle penetration, cone penetration experimental results may be more stable to test the AR binder with coarse CR. The cause is that the needle is easy to contact CR particles or not in experimental process, and CR particles have a relatively obvious influence on final penetration depth. However, the cone contacts CR particles with a high probability (97.28%) in experimental process and CR particles have little impact on penetration depth. At the same time, cone experiment is mainly based on the compressive property of larger contact area to evaluate the AR binder's consistency, which is more suitable for evaluating the AR binder with obvious elastic property.

(3) The dispersion of cone penetration experimental results is far less than that of needle penetration experiments for the AR binder with coarse CR (#40 mesh or lower). The standard deviations of needle penetration experimental results decrease gradually with the increase of the CR mesh number but are still slightly higher than that of cone penetration experiments.

Data Availability

All experiments data, models, and equations during the study are included within the article.

Conflicts of Interest

The authors declare that there are no conflicts of interest regarding the publication of this article.

Acknowledgments

The authors would like to acknowledge the financial support of the Natural Science Basic Research Plan in Shaanxi Province of China (no. 2018JM5049).

References

[1] T. Ma, Y. Zhao, X. Huang, and Y. Zhang, "Characteristics of desulfurized rubber asphalt and mixture," *KSCE Journal of Civil Engineering*, vol. 20, no. 4, pp. 1347–1355, 2016.

[2] J. Karger-Kocsis, L. Mészáros, and T. Bárány, "Ground tyre rubber (GTR) in thermoplastics, thermosets, and rubbers," *Journal of Materials Science*, vol. 48, no. 1, pp. 1–38, 2013.

[3] M. Sienkiewicz, K. Borzędowska-Labuda, S. Zalewski, and H. Janik, "The effect of tyre rubber grinding method on the rubber-asphalt binder properties," *Construction and Building Materials*, vol. 154, pp. 144–154, 2017.

[4] H. Wang, X. Liu, H. Zhang, P. Apostolidis, T. Scarpas, and S. Erkens, "Asphalt-rubber interaction and performance evaluation of rubberised asphalt binders containing non-foaming warm-mix additives," *Road Materials and Pavement Design*, vol. 21, pp. 1–22, 2020.

[5] M. Irfan, Y. Ali, S. Ahmed, and I. Hafeez, "Performance evaluation of crumb rubber-modified asphalt mixtures based on laboratory and field investigations," *Arabian Journal for Science and Engineering*, vol. 43, no. 4, pp. 1795–1806, 2018.

[6] S. Guo, Q. Dai, R. Si, X. Sun, and C. Lu, "Evaluation of properties and performance of rubber-modified concrete for recycling of waste scrap tire," *Journal of Cleaner Production*, vol. 148, pp. 681–689, 2017.

[7] S. Bressi, N. Fiorentini, J. Huang, and M. Losa, "Crumb rubber modifier in road asphalt pavements: state of the art and statistics," *Coatings*, vol. 9, no. 6, p. 384, 2019.

[8] P. Hao, Z. Li, and J. Xu, "Current standards for performance evaluation of rubberized asphalt," *Road Machinery & Construction Mechanization*, vol. 32, no. 6, pp. 47–52, 2015.

[9] American Society for Testing Materials, *ASTM D6114-19, Standard Specification for Asphalt-Rubber Binder*, American Society for Testing Materials, West Conshohocken, PA, USA, 2019.

[10] S.-C. Huang and A. T. Pauli, "Particle size effect of crumb rubber on rheology and morphology of asphalt binders with long-term aging," *Road Materials and Pavement Design*, vol. 9, no. 1, pp. 73–95, 2008.

[11] R. Yang, Y. Dang, and A. Li, "Study on quality evaluation index of rubber asphalt," *Highway*, vol. 6, pp. 174–178, 2009.

[12] T. Wang, R. Yang, A. Li, L. Chen, and B. Zhou, "Effects of Sasobit and its adding process on the performance of rubber asphalt," *Chemical Engineering Transactions*, vol. 51, pp. 181–186, 2016.

[13] A. Al-Omari, M. Taamneh, M. A. Khasawneh, and A. Al-Hosainat, "Effect of crumb tire rubber, microcrystalline synthetic wax, and nano silica on asphalt rheology," *Road Materials and Pavement Design*, vol. 21, pp. 1–23, 2020.

[14] N. S. Mashaan and M. R. Karim, "Waste tyre rubber in asphalt pavement modification," *Materials Research Innovations*, vol. 18, no. s6, pp. 6–9, 2014.

[15] China National Standards, *GB/T 16594, General Rules for Measurement of Length in Micron Scale by SEM*, China National Standards, Beijing, China, 2008.

[16] China National Standards, *GB/T 4509, Stand Test Method for Penetration of Bitumen*, China National Standards, Beijing, China, 2008.

[17] H. An, *Research on the Key Technologies for Application of Rubber Asphalt and its Mixture in Severe Cold Region*, Chang'an University, Xi'an, China, 2017.

[18] C. Guo, *Study on the Application Technology of Ground Tire Asphalt Rubber*, Chong'qing Jiaotong University, Chong'qing, China, 2008.

[19] S. Wang, Q. Wang, and S. Li, "Thermo oxidative aging mechanism of crumb-rubber-modified asphalt," *Journal of Applied Polymer Science*, vol. 133, no. 16, 2016.

[20] X. Wang and R. Cao, "Rubber asphalt modification mechanism," *Journal of Chang'an University (Natural Science Edition)*, vol. 31, no. 2, pp. 6–11, 2011.